Title:

Regional neuromuscular regulation within human rectus femoris muscle during gait

Authors:

Kohei Watanabe, Ph.D. [1], Motoki Kouzaki, Ph.D. [2], Toshio Moritani, Ph.D. [3]

Affiliations:

[1] School of International Liberal Studies, Chukyo University, Nagoya, Japan

[2] Laboratory of Neurophysiology, Graduate School of Human and Environmental Studies, Kyoto University, Kyoto, Japan

[3] Laboratory of Applied Physiology, Graduate School of Human and Environmental Studies, Kyoto University, Kyoto, Japan

Correspondence:

Kohei Watanabe, Ph.D.

School of International Liberal Studies, Chukyo University

Yagotohonmachi, Showa-ku, Nagoya, Japan 466-8666

Key words:

Neuromuscular compartment, Bi-articular muscles, Multi-channel surface electromyography

Total 4,060 words (Introduction to Acknowledgements)

Abstract

The spatial distribution pattern of neuromuscular activation within the human rectus femoris (RF) muscle was investigated during gait by multi-channel surface electromyography (surface EMG). Eleven healthy men walked on a treadmill with three gait speeds (4, 5, and 6 km/h) and gradients (0, 12.5, and 25°). The spatial distribution of surface EMG was tested by central locus activation (CLA), which is calculated from 2-D multi-channel surface EMG with 46 surface electrodes. For all conditions, CLA was around the middle regions during the swing-to-stance transition and moved in a proximal direction during the stance phase and stance-to-swing transition ($p < 0.05$). CLA during the stance-to-swing transition and early swing phase significantly moved to proximal site with increasing gait speed ($p < 0.05$). During the early stance and swing phases, with increasing grade, CLA significantly moved distally ($p < 0.05$). These results suggest that the RF muscle is regionally activated during a gait cycle and is non-uniformly regulated longitudinally.

Introduction

The rectus femoris (RF) muscle is one of the four components of quadriceps femoris muscle group and the only bi-articular muscle of the group, crossing the hip and knee joints. In gait analyses, the RF muscle has often been the subject of intense investigation, since it has been reported that an abnormality in regulation of neuromuscular activation of the RF muscle causes pathological gait in patients with upper motor neuron injuries such as stiff-legged (or –knee) gait (Chapman et al., 2008; Kerrigan et al., 1991; Reinbolt et al., 2008; Riley and Kerrigan, 1998; Sung and Bang, 2000). While numerous studies have investigated the neuromuscular activation pattern of the RF muscle during gait using electromyography (EMG) in able-bodied adults, children, the elderly, and patients (Annaswamy et al., 1999; Barr et al., 2010; Byrne et al., 2005; Chantraine et al., 2005; Di Nardo and Fioretti, 2013; Nene et al., 2004; Sung and Bang, 2000), little attention has been paid to the complicated anatomical characteristics of this muscle. It has been suggested that the RF muscle is comprised of two different muscle-tendon units or neuromuscular compartments, and this anatomical property is referred to as “muscle-within-muscle” (Balius et al., 2009; Gyftopoulos et al., 2008; Hasselman et al., 1995). Muscle fibers of the proximal one third and remainder of the RF muscle arise from two different proximal tendons which attach at the anterior inferior iliac spine and superior acetabular ridge, respectively (Balius et al., 2009; Gyftopoulos et al., 2008; Hasselman et al., 1995). Also, the proximal region and remainder of the human RF muscle are separately innervated by different motor nerve branches (Sung et al., 2003; Yang and Morris, 1999). Based on these

anatomical characteristics, it can be assumed that the two muscle-tendon units within the RF muscle are controlled via different strategies by the central nervous system and play different functional roles. A previous study also suggested that the two muscle-tendon units are independently and/or regionally activated during human movements (Hasselman et al., 1995). Currently, no solid experimental evidence exists regarding the quantitative as well as qualitative differences in neuromuscular activation among regions within the RF muscle during gait based on the specific anatomical characteristics.

Recent studies employed multi-channel surface EMG to record and assess the neuromuscular activation of large areas of the muscle (Holtermann et al., 2008; Staudenmann et al., 2009; Vieira et al., 2010; Watanabe et al., 2012). This technique would provide important information to understand the neural control of bi-articular muscles, the normal EMG pattern of the RF muscle during gait, and mechanisms of gait disorders in the elderly and/or disabled persons.

We investigated the neuromuscular activation of the whole RF muscle during gait using multi-channel surface EMG. We hypothesized that the RF muscle is regionally activated and non-uniformly regulated along its longitudinal line during gait because of the potential region-specific activation based on the anatomical properties (Balius et al., 2009; Gyftopoulos et al., 2008; Hasselman et al., 1995) .

Methods

Subjects

Subjects comprised 11 healthy men (age: 22.6 ± 2.5 years, height: 170.9 ± 6.6 cm, body mass: 66.7 ± 9.1 kg). We selected only male subjects because of thinner subcutaneous fat tissue than female subjects. They gave informed consent for the study after receiving a detailed explanation of the purposes, potential benefits, and risks associated with participation. All subjects were healthy with no history of any musculoskeletal or neurological disorders. All study procedures were in accordance with the Declaration of Helsinki and research code of ethics of Chukyo University and were approved by the Committee for Human Experimentation of the Graduate School of Human and Environmental Studies, Kyoto University.

Experimental design

Subjects walked on a treadmill (MEDTRACK ST65, Quinton Instrument Co., WA, USA) set with five different combinations of various speeds and grades: 1) 4 km/h at a grade of 0°, 2) 5 km/ h at a grade of 0°, 3) 6km/h at a grade of 0°, 4) 5 km/h at a grade of 12.5°, and 5) 5 km/h at a grade of 25°. To investigate possible region-specific neuromuscular responses during gait, various speeds and grades were given in the present study. Each task involved a phase with a gradual increase in speed and/or grade for 15-20 s until reaching the specified conditions, which were then maintained for 30-45 s. Rest periods among the trials under the different conditions were ≥ 2 min.

Multi-channel surface EMG recording

Multi-channel surface EMG signals were recorded from the RF muscle of the left thigh with a matrix of 48 surface electrodes comparing 2 columns and 24 rows (1 x 5 mm, 10-mm inter-electrode distance) (ELSH004, OT Bioelectronica, Torino, Italy) (Fig. 1). This electrode arrangement is similar to that in our previous study (Watanabe et al., 2013). Since region-specific neuromuscular activation was mainly demonstrated along the RF muscle longitudinally in our previous studies (Watanabe et al., 2012; Watanabe et al., 2013; Watanabe et al., 2014), electrodes were also arranged longitudinally. A conductive gel was applied within the cavities of the grid electrodes to ensure appropriate skin contact. Prior to attaching the electrode grid, the skin was shaved, abraded, and cleaned with alcohol. To determine electrode positions, the edge of the superficial region of the RF muscle was identified using ultrasonography (FAZONE CB, FUJI FILM, Tokyo, Japan). The ultrasonographic procedure to determine electrode positions was similar to that employed in our previous studies (Watanabe et al., 2012; Watanabe et al., 2013; Watanabe et al., 2014). On real-time axial ultrasonographic images, the border between the RF muscle and neighboring muscles, i.e. vastus lateralis, vastus medialis, sartorius, and tensor fasciae latae muscles, was identified, and marks were applied to the skin above the border using a felt-tip pen. Consequently, superficial regions of the RF muscle were surrounded by the marks on the skin, and electrodes were attached within them. During this procedure, subjects' hip and knee joint angles

were both 90° (180° is fully extended). The columns of electrodes were placed on the longitudinal axis of the RF muscle along a line between the anterior superior iliac spine and the superior edge of the patella. The line between these two points was defined as the longitudinal line of the RF muscle based on anatomical data on the human RF muscle (Sung et al., 2003; Yang and Morris, 1999). The center of the second electrodes from the proximal side placed in the proximal third along the longitudinal line of the RF muscle (Fig. 1). A reference electrode was placed at the iliac crest. In our previous study, we confirmed that multi-channel surface EMG of the RF muscle, which was recorded with this procedure, demonstrated a region-specific activation pattern similar to intramuscular EMG pattern from multiple regions of the muscle (Watanabe et al., 2012).

Monopolar EMG signals were amplified by a factor of 1,000, sampled at 2,048 Hz with an 8^{th} order Bessel band pass filter at 10-750 Hz (anti-aliasing filter), and converted to digital form by a 12-bit analog-to-digital converter (EMG-USB, OT Bioelectronica, Torino, Italy). Monopolar surface EMG signals were off-line band-pass filtered (20 - 400 Hz) and transferred to analysis software (MATLAB 7, MathWorks GK, Tokyo, Japan). The high pass frequency was set at 20 Hz in order to remove motion artifacts (De Luca et al., 2010). From the electrode pairs between neighboring electrodes along the rows, bipolar surface EMG signals were calculated (Watanabe et al., 2013). Since we used two lines of 6 x 4 array electrodes in this study, 36 bipolar surface EMG signals were obtained (3 pairs x 6 array electrodes x 2 lines) (Fig. 1).

For analysis of surface EMG, timings of heel contact and toe-off were identified by signals from footswitches taped to the heel and toe of the left foot. Electrical signals from the footswitches were synchronized with surface EMG signals using an analog-to-digital converter. One heel contact to the next heel contact was determined as one step and considered as 100% of a gait cycle for each stride. During the constant phase of each trial, 20 consecutive strides were sampled for analysis. The root mean square (RMS) of surface EMG was calculated from the sampled surface EMG signal. To average and normalize RMS values, the following procedure was performed: 1) for each gait condition, each electrode pair and each subject, RMS values were averaged every 2% of a stride across the 20 strides; 2) RMS values of the same rows were averaged for each subject and gait condition; 3) for each subject and gait condition, the peak RMS value was determined from 50 averaged RMS values of each 2% of a gait cycle; 4) RMS values for each 2% of a gait cycle were normalized by the peak value for each subject and gait condition. Consequently, 18 normalized RMS values were obtained at every 2% of a gait cycle, defined as CH1 to CH18 from the proximal side (Fig. 1). To quantify the spatial distribution of RMS within the muscle, central locus activation (CLA) was also calculated at every 2% of a gait cycle. CLA was calculated as the centroid of the normalized RMS along the longitudinal line of the muscle in inter-electrode distance units. Since we used an array electrode with four electrodes, there were blanks between arrays where we were unable to detect a surface EMG signal. For CLA calculation, these blanks were

considered and the results are shown as the distance (cm) from the most proximal edge of electrodes. Therefore, for calculating CLA we added the averaged values between CH3 and 4, CH and 7,…, CH15 and 16 as the estimated RMS values between arrays.

Statistics

Non-parametric tests were employed since the sample size was not large (n=11) and data distribution was partly non-Gaussian. CLA values at every 2% of a gait cycle were equally divided into ten phases. In each gait phase, CLA values were compared among the different speeds and grades using the Wilcoxon rank sum test. For each condition, CLA values in individual gait phases were compared with the CLA value in gait phase 1 using the Wilcoxon rank sum test. Cadence and the timing of toe-off were compared among conditions using Wilcoxon rank sum test. The level of significance was set at 0.05 and modified by Bonferroni correction, i.e., $\alpha = 0.05$/number of pairs. Statistical analyses were performed using SPSS software (version 15.0; SPSS, Tokyo, Japan).

Results

The mean cadence and timing of toe-off for each condition are shown in Table 1. There were significant differences in cadence among the different speeds and grades and in the timing of toe-off between 5 and 6km/h at 0° of grades ($p < 0.05$) (Table 1).

Mean absolute and normalized RMS patterns from different channels along the

longitudinal line of the RF muscle at every 2% of gait cycle are shown in Figs. 2 and 3. For the three different speeds, two bursts are demonstrated near the point of heel contact (90-20% of gait cycle) and toe-off (approximately 60% of gait cycle) for all channels. The first (90-20% of gait cycle) and second (approximately 60% of gait cycle) bursts seemed to be relatively larger in the distal and proximal compared to other regions, respectively (Fig. 3). In fact, normalized RMS values in proximal regions (CH1-6) were approximately 0.5~0.6 during 90-20% of gait cycle and 0.6~0.7 near 60% (Fig. 3). On the other hand, normalized RMS values in distal regions (CH13-18), were 0.8~0.9 during 90-20% of gait cycle and 0.2~0.3 near 60% (Fig. 3). In proximal regions such as CH1-6, a slight increase in normalized RMS values with an increase in speed was seen before toe-off, at approximately 50-60% of gait cycle (Fig. 3). For upslope conditions, additional peak activation during the swing phase was observed in the middle to proximal regions and increase of these bursts was seen with increasing in grade at the proximal regions (Fig. 3 and 4). Also, an increase in normalized RMS values with increasing grade was seen after heel contact, at approximately 0-10% of gait cycle, in distal regions (Fig. 3).

For visualization, the mean normalized RMS is illustrated as a color scale map with the CLA position (Fig. 4). Heterogeneous spatial distributions of normalized RMS values are demonstrated along the longitudinal line of the muscle during a gait cycle for all conditions. Under all conditions, CLA is located near the center of the muscle during a gait cycle and moves

proximally from heel contact to toe-off.

Figure 5 shows CLA during a gait cycle with different speeds and grades. CLA for all conditions significantly shifted from the middle to proximal sides from heel contact (gait phases 10-1) to the swing phase (gait phases 7-9) ($p < 0.05$) (Fig. 5). In gait phases 6-8, CLA for 5 km/m with 0° was significantly located more proximally than for 4 km/m with 0° ($p < 0.05$) (Fig. 5A). CLA for 6 km/h with 0° was significantly more proximal than for 5 km/m with 0° in gait phase 9 ($p < 0.05$) (Fig. 4A). For 5 km/h with 12.5°, CLA in gait phases 1-3 and 7-8 was significantly located more distally when compared to 5 km/h with 0°($p < 0.05$) (Fig. 5B). In gait phase 9, CLA for 5 km/h with 25° was significantly located more distally than 5 km/h with 0° ($p < 0.05$) (Fig. 5B).

Discussion

The present study investigated neuromuscular activation in a large area of the RF muscle based on high-resolution spatial information from surface EMG. The main findings of this study were that CLA, which is an indicator of the spatial distribution of surface EMG responses within the muscle, changed significantly during a gait cycle and with an increasing gait speed and grade. These results support our hypothesis that the RF muscle is regionally activated and non-uniformly regulated longitudinally during gait. The results can also be explained by the anatomical properties (Balius et al., 2009; Gyftopoulos et al., 2008; Hasselman et al., 1995). Also, the present study

confirmed that region-specific neuromuscular activation within the RF muscle occurs during human locomotion as well as isometric contractions (Watanabe et al., 2012; Watanabe et al., 2013; Watanabe et al., 2014).

CLA moved during a gait cycle, suggesting that surface EMG responses of the whole RF muscle are not uniform during gait movement. Under all conditions, during the swing-to-stance transition (gait phases 10 and 1) and early stance phase (gait phase 2), CLA was located between middle and distal parts of the muscle (approximately 13 cm from the most proximal electrode) (Fig. 5). Although the bursts were observed through all regions during these phases (gait phases 10-2), the relative intensity of the bursts around the middle and distal regions was higher than in proximal regions (Fig. 3). This non-uniformity in the normalized RMS along the longitudinal line of the muscle was reflected in the result of CLA around the point of heel contact (Fig. 5). There remained a delayed first burst (Fig. 2-4) with no activations in the middle and distal regions during the stance phase (gait phases 2-5), leading to a CLA shift from the middle to proximal sites (Figs. 4 and 5). During the stance-to-swing transition (gait phase 6), second bursts were demonstrated at all regions and relatively higher RMS values were observed in the middle to proximal regions as compared with the middle to distal regions (Figs. 2-4). A prolonged second burst in the early swing phase (gait phases 7-8) besides the relatively higher second burst during stance-to-swing transition in the middle to proximal regions would lead to a significant shift of CLA in a proximal direction during gait

phases 6-8 ($p < 0.05$) (Fig. 5). The important point to note here is that different spatial distribution patterns of the normalized RMS along the longitudinal line of the RF muscle were observed between the first and second bursts. This was reflected as significant differences in CLA between gait phase 1 and phases 6-7 ($p < 0.05$) (Fig. 5). The largest knee extension joint torque starts just after the swing-to-stance transition and the directions of joint moment change from extension to flexion of the hip joint during stance-to-swing transition (Lay et al., 2006). Since the RF muscle contributes to knee extension and hip flexion joint movement, Annaswamy et al. (Annaswamy et al., 1999) proposed that the RF muscle acts as a knee extensor for load-bearing during the first burst and hip flexor for propelling the limb forward into the swing during the second burst. Therefore, we assumed that the differences in CLA and/or spatial distribution patterns of the normalized RMS between the phases with the first and second bursts reflect the region-specific functional roles within the RF muscle. Recent studies (Hagio et al., 2012; Watanabe et al., 2012; Watanabe et al., 2014) suggested the heterogeneity of functional roles along the longitudinal line of the RF muscle. Hagio et al. (Hagio et al., 2012) reported a selective contribution of the proximal regions of the RF muscle to hip flexion joint torque using intramuscular electrical stimulation-induced "involuntary" contraction. During "voluntary" isometric contractions, we also demonstrated relatively similar activations among the regions for knee extension and the relatively higher activation in the proximal compared to other regions for hip flexion using multi-channel surface EMG and intramuscular EMG

(Watanabe et al., 2012). From these previous studies, there may be differences in superiority to knee extension and hip flexion joint moments along the longitudinal line of the RF muscle. Spatial distribution patterns of the normalized RMS during gait observed in the present study can be explained based on the results of these previous studies (Hagio et al., 2012; Watanabe et al., 2012; Watanabe et al., 2014). We assumed that the whole RF muscle acts as a knee extensor during swing-to-stance transition, and the proximal to middle regions act as a hip flexor during stance-to-swing transition.

A previous study demonstrated that, with increasing gait speed, there is an increase in the EMG amplitude of the RF muscle during the stance-to-swing transition and early swing phase (van Hedel et al., 2006). In the present study, CLA during these phases moved to the proximal sites (Fig. 5), meaning that gait speed-related changes in EMG were regionally observed within the RF muscle. While we did not measure changes in joint moments with an increase in gait speed, it seems reasonable that hip, knee, and ankle joint moments during gait increase with a rise in gait speed. Thus, we assumed that the proximal regions dominantly contribute to an increase in hip flexion joint moment with increasing gait speed. This assumption is based on the above-mentioned studies (Hagio et al., 2012; Watanabe et al., 2012; Watanabe et al., 2014) that showed the potential region-specific functional role within the RF muscle. Also, our results suggest that the regional neuromuscular activation patterns within the RF muscle are potentiated by an increasing gait speed.

In the present study, during the early stance (gait phases 1-3) and swing phases (gait phases 7-9), CLA with a grade of 12.5° or 25° was significantly located at a more distal site than at 0° ($p < 0.05$) (Fig. 5B). Former change may be partly explained by an increase in knee joint extensor moment during early stance phase with an increase in the floor grade (Lay et al., 2006). Our previous study suggested that contribution of distal regions to knee extension joint moment is higher than other regions (Watanabe et al., 2012). However, latter change was difficult to explain with joint kinematics and/or kinetics. For 12.5° and 25°, a third burst was observed in the proximal regions before the second burst, i.e., the stance-to-swing transition (Figs. 2, 3, and 4). Lay et al. showed change in hip joint moment pattern during the stance-to-swing transition with an increase in the floor grade (Lay et al., 2006). We speculated this additional burst in the proximal regions relate to changes in hip joint kinetics. These results suggest that the RF muscle is not uniformly regulated in response to changes in the floor grade as well as gait speed during gait.

During gait, the RF muscle deforms with changes in hip and knee joints and its own contraction. This will lead to changes in the distance between electrodes and the origin of the surface EMG signal, i.e., innervation zone (IZ), and/or in the relative alignment between a pair of electrodes and muscle fibers (Farina, 2006; Farina et al., 2001). However, we could not quantify these effects on our results. This is major limitation of our study, and we should be careful interpreting the present results. In some previous studies, the potential effect of cross-talk on

surface EMG signals of the RF muscle were well documented (Barr et al., 2010; Byrne et al., 2005; Di Nardo and Fioretti, 2013; Nene et al., 2004). While our previous study demonstrated a similar trend in RMS between surface and intramuscular (wire electrode) EMG detected in proximal, middle, and distal regions of the RF muscle during isometric contractions (Watanabe et al., 2012), the effect of cross-talk was not investigated during gait. We should note that surface EMG signals from the RF muscle in the present study may include cross-talk from adjacent muscles.

The normal EMG pattern of the RF muscle during gait was discussed in recent studies (Barr et al., 2010; Byrne et al., 2005; Di Nardo and Fioretti, 2013; Nene et al., 2004). Two main burst patterns, one occurring around swing-to-stance transition and the second occurring around stance-to-swing transition, comprise the normal activation pattern of the RF muscle during gait (Annaswamy et al., 1999; Winter and Yack, 1987; Yang and Winter, 1985). In the present study, this pattern was seen in the whole muscle at all gait speed with level walking (Fig. 2 and 3). However, recent studies revealed one burst around stance-to-swing transition in the RF muscle by intramuscular EMG (Barr et al., 2010; Nene et al., 2004). They pointed out that differences in EMG patterns in the literature can be explained by methodological issues in surface EMG, such as cross-talk, since the burst around swing-to-stance transition was shown by surface but not intramuscular EMG (Nene et al., 2004). In the present discussion, we should not overlook the fact that, while Annaswamy et al. (Annaswamy et al., 1999) detected intramuscular EMG from proximal,

middle, and distal regions of the RF muscle and averaged the signals from the three regions, Nene et al. (Nene et al., 2004) recorded intramuscular EMG from the middle site of the RF muscle. From the results of the present study, we suggested that the EMG pattern variation of the RF muscle in the literature can be partly explained by the potential region-specific functional role or neuromuscular activation within the muscle. Also, based on our findings, we suggest that the careful determination of electrode positions or multi-channel recording may resolve this issue.

Previous studies reported that RF muscle activity is closely associated with stiff-legged (or -knee) gait (Chapman et al., 2008; Kerrigan et al., 1991; Knuppe et al., 2013; Reinbolt et al., 2008; Riley and Kerrigan, 1998; Sung and Bang, 2000). It has been suggested that hyperactivity of the RF muscle during stance-to-swing transition decreases knee flexion and thereby impairs toe clearance. This pathological gait pattern is seen in the patients with upper motor neuron injuries resulting from stroke, traumatic brain injury, spinal cord injury, cerebral palsy, or multiple sclerosis. For the treatment of stiff-legged gait, distal transfer or motor nerve block of the RF muscle has been applied in order to reduce the action of the muscle (Chantraine et al., 2005; Sung and Bang, 2000). In the present study, the proximal regions of the RF muscle were regionally activated during stance-to-swing transition and swing (Figs. 2, 3, and 4). Based on this, assessment of the heterogeneity of spatial distribution in neuromuscular activation within the RF muscle in addition to information on the hamstring muscles and kinematic parameters may further understanding of the

mechanism and suggest novel treatments for the stiff-legged (or –knee) gait.

In conclusion, we investigated neuromuscular activation of the whole RF muscle during gait using multi-channel surface EMG. The spatial distribution of surface EMG along the longitudinal line of the RF muscle changed through a gait cycle. Also, effects of alterations in the gait speed and grade were regionally observed within the muscle. These results suggest that the RF muscle is regionally activated and may be non-uniformly regulated longitudinally during gait.

Acknowledgement

This research was supported in part by JSPS KAKENHI, a Grant-Aid for Research Activity Start-up (No. 24800071).

Conflict of interest

The authors have no conflicts of interest related to this study.

References

Annaswamy, T. M., Giddings, C. J., Della Croce, U. and Kerrigan, D. C., 1999. Rectus femoris: its role in normal gait. Archives of Physical Medicine and Rehabilitation 80, 930-4

Balius, R., Maestro, A., Pedret, C., Estruch, A., Mota, J., Rodriguez, L., Garcia, P. and Mauri, E., 2009. Central aponeurosis tears of the rectus femoris: practical sonographic prognosis. British Journal of Sports Medicine 43, 818-24

Barr, K. M., Miller, A. L. and Chapin, K. B., 2010. Surface electromyography does not accurately reflect rectus femoris activity during gait: impact of speed and crouch on vasti-to-rectus crosstalk. Gait and Posture 32, 363-8

Byrne, C. A., Lyons, G. M., Donnelly, A. E., O'Keeffe, D. T., Hermens, H. and Nene, A., 2005. Rectus femoris surface myoelectric signal cross-talk during static contractions. Journal of Electromyography and Kinesiology 15, 564-575

Chantraine, F., Detrembleur, C. and Lejeune, T. M., 2005. Effect of the rectus femoris motor branch block on post-stroke stiff-legged gait. Acta Neurologica Belgica 105, 171-7

Chapman, A. R., Vicenzino, B., Blanch, P. and Hodges, P. W., 2008. Patterns of leg muscle recruitment vary between novice and highly trained cyclists. Journal of Electromyography and Kinesiology 18, 359-371

De Luca, C. J., Gilmore, L. D., Kuznetsov, M. and Roy, S. H., 2010. Filtering the surface EMG signal: Movement artifact and baseline noise contamination. Journal of Biomechanics 43, 1573-9

Di Nardo, F. and Fioretti, S., 2013. Statistical analysis of surface electromyographic signal for the assessment of rectus femoris modalities of activation during gait. Journal of Electromyography and Kinesiology 23, 56-61

Farina, D., 2006. Interpretation of the surface electromyogram in dynamic contractions. Exercise and Sport Sciences Reviews 34, 121-7

Farina, D., Merletti, R., Nazzaro, M. and Caruso, I., 2001. Effect of joint angle on EMG variables in leg and thigh muscles. IEEE Engineering in Medicine and Biology Magazine 20, 62-71

Gyftopoulos, S., Rosenberg, Z. S., Schweitzer, M. E. and Bordalo-Rodrigues, M., 2008. Normal anatomy and strains of the deep musculotendinous junction of the proximal rectus femoris: MRI features. AJR. American Journal of Roentgenology 190, W182-6

Hagio, S., Nagata, K. and Kouzaki, M., 2012. Region specificity of rectus femoris muscle for force vectors in vivo. Journal of Biomechanics 45, 179-82

Hasselman, C. T., Best, T. M., Hughes, C. t., Martinez, S. and Garrett, W. E., Jr., 1995. An explanation for various rectus femoris strain injuries using previously undescribed muscle architecture. American Journal of Sports Medicine 23, 493-9

Holtermann, A., Gronlund, C., Karlsson, J. S. and Roeleveld, K., 2008. Differential activation of regions within the biceps brachii muscle during fatigue. Acta Physiol (Oxf) 192, 559-67

Kerrigan, D. C., Gronley, J. and Perry, J., 1991. Stiff-legged gait in spastic paresis. A study of quadriceps and hamstrings muscle activity. American Journal of Physical Medicine and Rehabilitation 70, 294-300

Knuppe, A. E., Bishop, N. A., Clark, A. J., Alderink, G. J., Barr, K. M. and Miller, A. L., 2013. Prolonged swing phase rectus femoris activity is not associated with stiff-knee gait in children with cerebral palsy: a retrospective study of 407 limbs. Gait and Posture 37, 345-8

Lay, A. N., Hass, C. J. and Gregor, R. J., 2006. The effects of sloped surfaces on locomotion: a kinematic and kinetic analysis. Journal of Biomechanics 39, 1621-8

Nene, A., Byrne, C. and Hermens, H., 2004. Is rectus femoris really a part of quadriceps? Assessment of rectus femoris function during gait in able-bodied adults. Gait and Posture 20, 1-13

Reinbolt, J. A., Fox, M. D., Arnold, A. S., Ounpuu, S. and Delp, S. L., 2008. Importance of preswing rectus femoris activity in stiff-knee gait. Journal of Biomechanics 41, 2362-9

Riley, P. O. and Kerrigan, D. C., 1998. Torque action of two-joint muscles in the swing period of stiff-legged gait: a forward dynamic model analysis. Journal of Biomechanics 31, 835-40

Staudenmann, D., Kingma, I., Daffertshofer, A., Stegeman, D. F. and van Dieen, J. H., 2009. Heterogeneity of muscle activation in relation to force direction: a multi-channel surface electromyography study on the triceps surae muscle. Journal of Electromyography and Kinesiology 19, 882-95

Sung, D. H. and Bang, H. J., 2000. Motor branch block of the rectus femoris: its effectiveness

in stiff-legged gait in spastic paresis. Archives of Physical Medicine and Rehabilitation 81, 910-5

Sung, D. H., Jung, J. Y., Kim, H. D., Ha, B. J. and Ko, Y. J., 2003. Motor branch of the rectus femoris: anatomic location for selective motor branch block in stiff-legged gait. Archives of Physical Medicine and Rehabilitation 84, 1028-31

van Hedel, H. J., Tomatis, L. and Muller, R., 2006. Modulation of leg muscle activity and gait kinematics by walking speed and bodyweight unloading. Gait and Posture 24, 35-45

Vieira, T. M., Merletti, R. and Mesin, L., 2010. Automatic segmentation of surface EMG images: Improving the estimation of neuromuscular activity. Journal of Biomechanics 43, 2149-58

Watanabe, K., Kouzaki, M. and Moritani, T., 2012. Task-dependent spatial distribution of neural activation pattern in human rectus femoris muscle. Journal of Electromyography and Kinesiology 22, 251-8

Watanabe, K., Kouzaki, M. and Moritani, T., 2013. Region-specific myoelectric manifestations of fatigue in human rectus femoris muscle. Muscle and Nerve 48, 226-234

Watanabe, K., Kouzaki, M. and Moritani, T., 2014. Non-uniform surface EMG responses to change in joint angle within rectus femoris muscle. Muscle and Nerve in press

Winter, D. A. and Yack, H. J., 1987. EMG profiles during normal human walking: stride-to-stride and inter-subject variability. Electroencephalography and Clinical Neurophysiology 67, 402-11

Yang, D. and Morris, S. F., 1999. Neurovascular anatomy of the rectus femoris muscle related to functioning muscle transfer. Plastic and Reconstructive Surgery 104, 102-6

Yang, J. F. and Winter, D. A., 1985. Surface EMG profiles during different walking cadences in humans. Electroencephalography and Clinical Neurophysiology 60, 485-91

Table 1

Cadence and toe-off timing for each condition.

Values are mean and SD. * $p < 0.05$ vs 5km/h with 0 deg.

Speed (km/h)	Grade (°)	Cadence (bpm)	Toe off timing (% gait cycle)
4	0	109.2 ± 4.5 *	59.5 ± 1.5
5	0	119.7 ± 4.3	58.5 ± 2.2
6	0	129.6 ± 4.9 *	57.4 ± 2.0 *
5	12.5	122.6 ± 4.8 *	59.3 ± 1.8
5	25	130.0 ± 8.8 *	54.7 ± 15.4

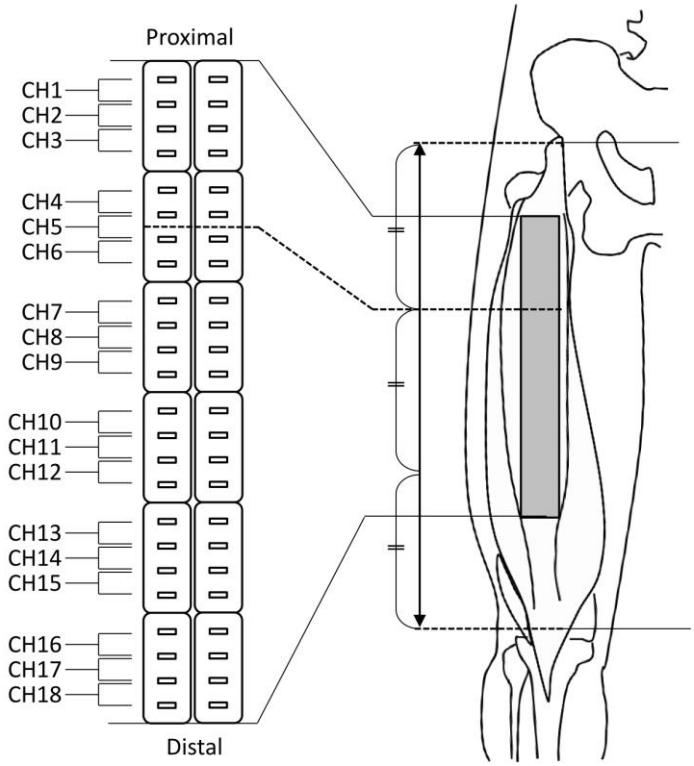

Fig. 1

Electrode positions and definitions of channel numbers for the rectus femoris muscle.

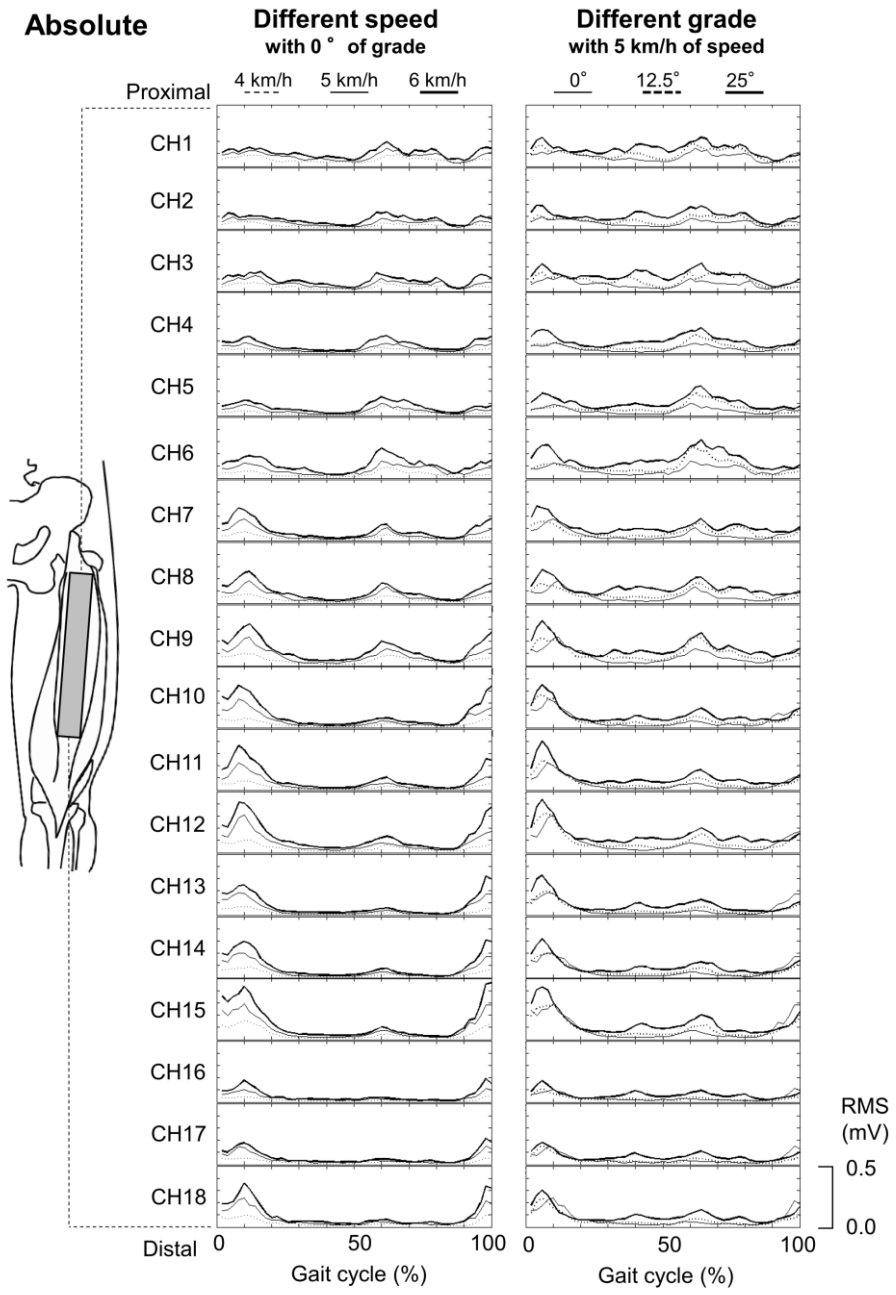

Fig. 2

Mean absolute root mean square values of multi-channel surface electromyography for all subjects at different channels along the longitudinal line of the rectus femoris muscle for various gait speeds (left panel) and surface grades (right panel). In the left panel, dashed, solid, and thick solid lines indicate gait speeds of 4, 5, and 6 km/h with a 0°grade, respectively. In the right panel, solid, dashed and thick solid lines indicate a gait speed of 5 km/h with grades of 0, 12.5, and 25 °.

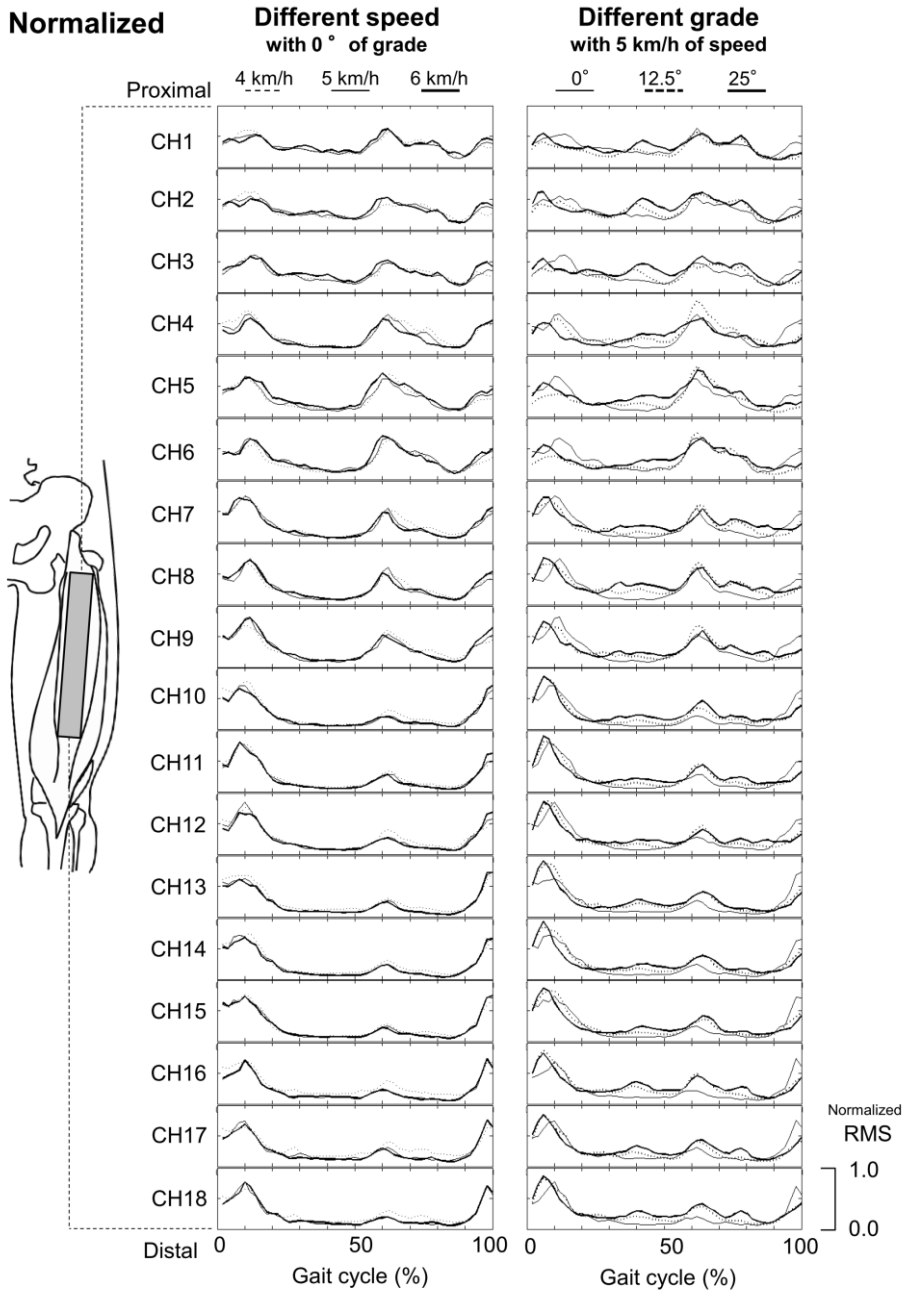

Fig. 3

Mean normalized root mean square values of multi-channel surface electromyography for all subjects at different channels along the longitudinal line of the rectus femoris muscle for various gait speeds (left panel) and surface grades (right panel). In the left panel, dashed, solid, and thick solid lines indicate gait speeds of 4, 5, and 6 km/h with a 0°grade, respectively. In the right panel, solid, dashed and thick solid lines indicate a gait speed of 5 km/h with grades of 0, 12.5, and 25 °.

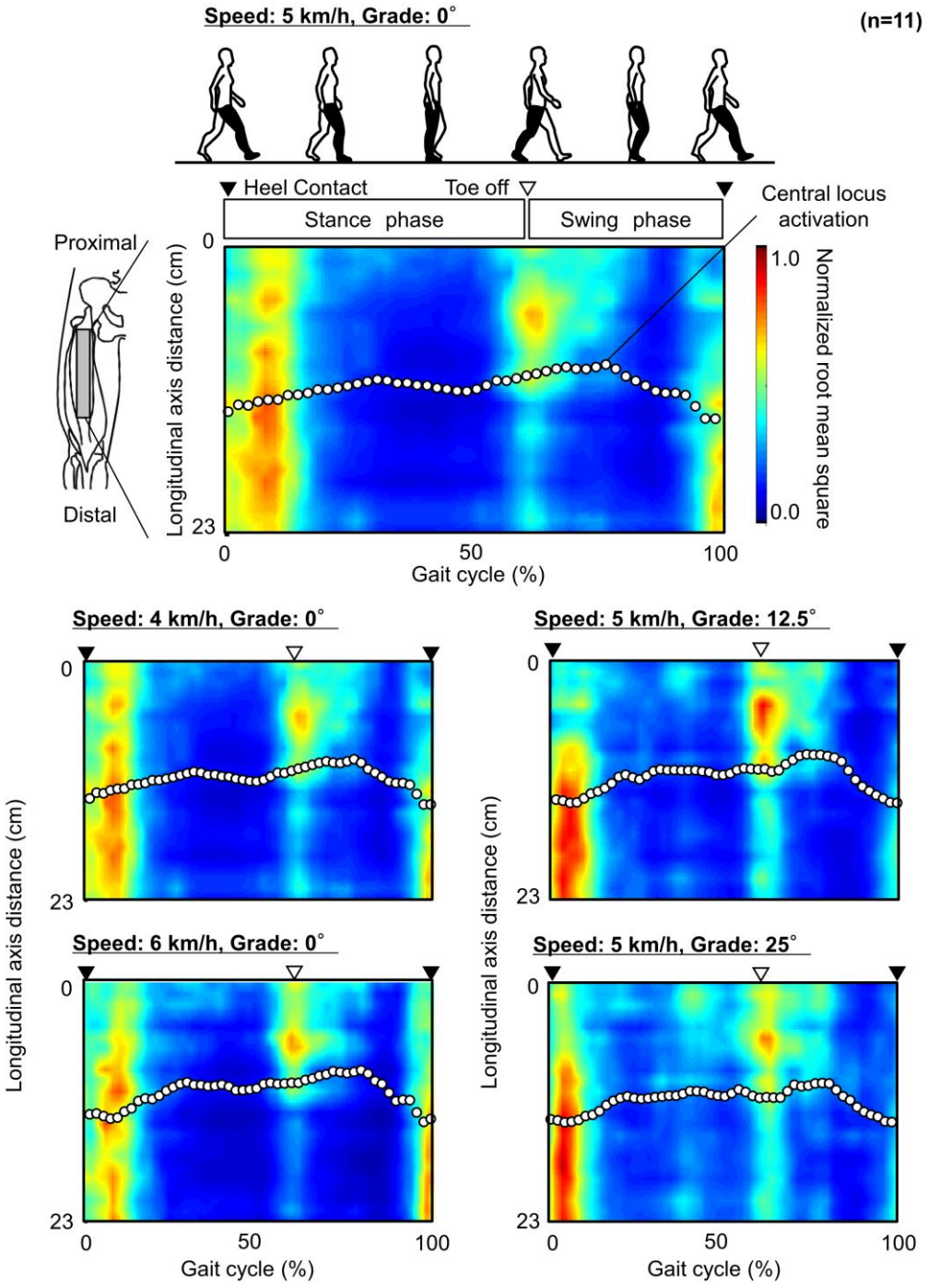

Fig. 4

Mean normalized root mean square values of multi-channel surface electromyography along the longitudinal line of the rectus femoris muscle shown by a color map for various gait conditions. Dark red corresponds to the highest normalized root mean square value, and blue indicates a lower value. Filled and unfilled triangles are timings for heel contact and toe-off, respectively.

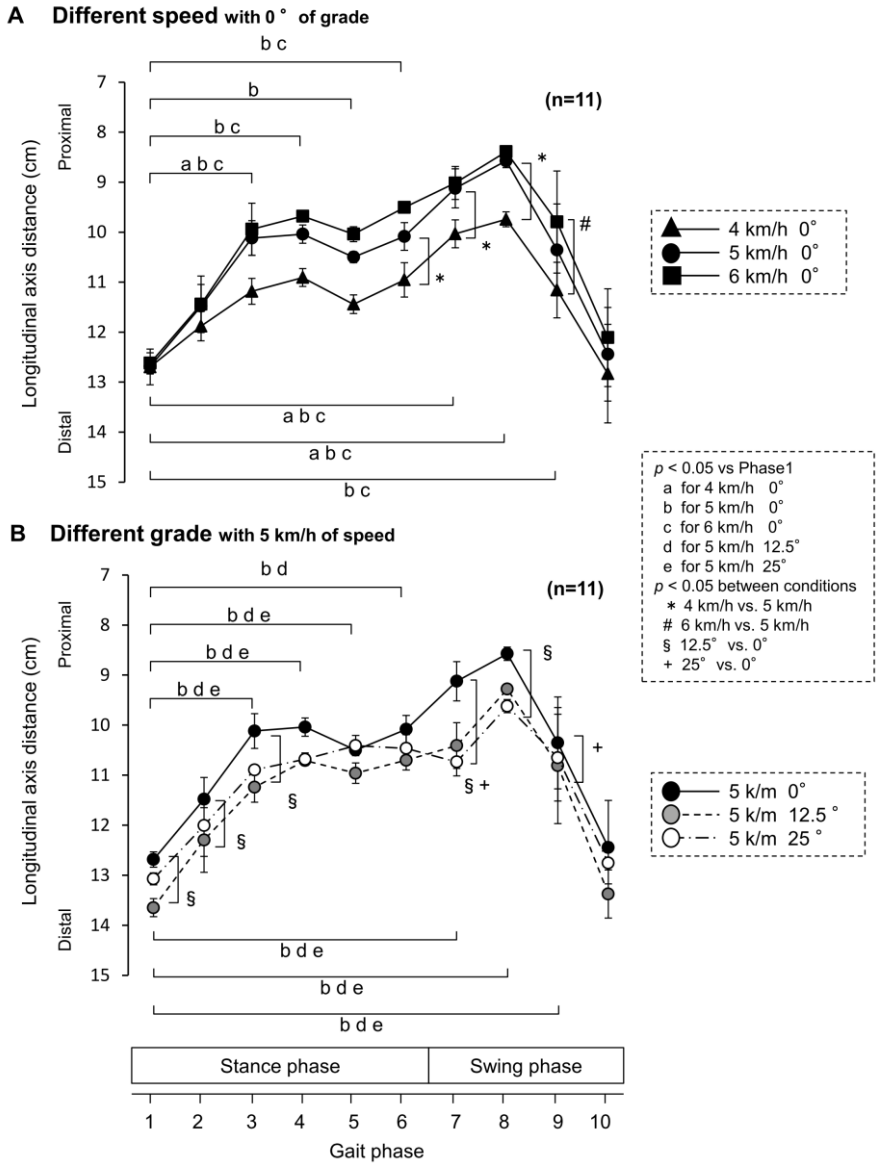

Fig. 5

Mean central locus activation (CLA) for different gait speeds (A) and grades (B). The closed triangle, closed circle, and closed square, represent the values for 4, 5, and 6 km/h gait speeds with a grade of 0°, respectively. (A) Black, gray, and white circles indicate the values for a 5 km/h gait speed with grades of 0, 12.5, and 25° of grade, respectively. (B) Error bars indicate standard deviations. a, b, c, d, and e indicate $p < 0.05$ vs. values for gait phase 1 for 4, 5, and 6 km/h with 0° and 5 km/h with 12.5 and 25°. *, #, §, and + indicate $p < 0.05$ between the values for 5 km/h with 0°vs. those for 4 km/h with 0°, the values for 5 km/h with 0° vs. those for 6 km/h with 0°, the values for 5 km/h with 0° vs. those for 5 km/h with 12.5 °, and the values for 5 km/h with 0° vs. those for 5 km/h with 25 °, respectively.